Computer Assisted Mechanics and Engineering Sciences, 11: 211–222, 2004.

Discrete model of twisted rings

Zsolt Gáspár* and Róbert Németh**
*HAS-Research Group for Computational Structural Mechanics,
**Department of Structural Mechanics,
Budapest University of Technology and Economics,
H-1521 Budapest, Műegyetem rkp. 3., Hungary
*gaspar@ep-mech.me.bme.hu, **nemeth.robert@gmx.net

(Received April 2, 2003)

A discrete model consisting N straight links and N springs is defined. The originally straight model is bent into a discrete torus, then it is twisted. The C_2 symmetric shapes can be determined by four parameters, and there are three constrains. The equilibrium paths are determined by the simplex method (piecewise linear approximation). Global bifurcation diagrams, spatial equilibrium shapes and parasitic solutions are analysed.

1. Introduction

Let us consider a rod with circular cross-section of radius r. The rod is long (i.e. $L \gg r$, where L is the length of the rod) and initially straight. The rod is made of a homogenous, linear elastic material with the modulus of elasticity E and the shear modulus of elasticity G. Bending stiffness is characterized by the constant $A = EI_x$, where $I_x = \dfrac{r^4\pi}{4}$, and the twist stiffness by $C = GI_p$, where $I_p = \dfrac{r^4\pi}{2}$. The rod is supposed to be inextensible and unshearable. Recently many publications [1–5, 8, 10, 11] deal with the following problem: first the rod is bent to a torus with a pair of moments acting on its end-sections. Then the end-sections are twisted around the rod axis, continuously providing their contact. The increasing twist rate causes stability loss at a special value, and then spatial equilibrium states are observable.

This model is widely used as a mechanical model of DNA molecules, but several simplifications are made. In one of these simplifications the rod is treated as penetrable, i.e. we do not deal with the contact problem. The symmetry properties of such solutions are classified by Domokos [4]. When the impenetrable rod is examined, the situation is sophisticated. In simple cases contact points, at higher values of twist rate contact line(s) and points arise [1]. There is an interval of twist rate, where only contact line arises [8]. The contact can even break the symmetries shown by Domokos. Not all of the equilibrium states are stable, of course. The stability of solutions was examined by Coleman et al. [1].

The explicit solution of the system of differential equations of the elastic rod is given by Swigon et al. [10]. This solution is expressed in terms of elliptic integrals, what makes its handling relatively difficult, if we need the co-ordinates of all points of the rod-axis. (This is the case e.g. if we are looking for contact points). The extension of the solution to shearable or extensible rod is also complex. The DNA itself build up from discrete base pairs, which can be modeled by linear elements connected by springs. (Discrete models give good approximations to the solution of the continuous model, however the solution set is often richer, than that of the continuous model. A good example is shown in [9], where Euler's rod was examined.) A naturally discrete model of the DNA o-ring is developed by Coleman et al. in [2].

For the sake of simplicity we are dealing with the mathematical problem, so we do not care about the contact points and lines, we assume, the rod is penetrable. That means we will approximate the deformation of a line of length L, which has a finite bending and twisting stiffness. The radius r has no effect on the further computations.

2. The discrete model

The discrete model of the rod consist of N straight rigid links of equal length l ($l = L/N$). The links are numbered from 1 to N. Each link is connected to the next one with a 0 dimensional spring. Each spring has the number of the previous link. We consider a spring (the Nth) between the Nth and the first links with the same spring coefficient as the other springs have. (So a virtual $N+1$th link would take up the same geometrical place as the first link.)

Of course, the elements in the discrete model are inextensible and unshearable, just like in the continuous model. The twist stiffness of the links is equal to the rod's twist stiffness (C). The springs are infinitely stiff against the twist, while for bending every spring in any direction has the same stiffness $c = A/l$.

In our computations we will use two levels of left handed reference systems. The first one is the local $\xi_{i,s}$, $\eta_{i,s}$, $\zeta_{i,s}$ system, which is fixed to a cross-section in the ith link, at a distance s from its starting point. So the starting cross-section for the ith link has the coordinate system $\xi_{i,0}$, $\eta_{i,0}$, $\zeta_{i,0}$, and the end-section has the system $\xi_{i,l}$, $\eta_{i,l}$, $\zeta_{i,l}$. The axes $\eta_{i,s}$ and the $\zeta_{i,s}$ are lying in the plane of cross-section, $\xi_{i,s}$ is collinear with the link's axis and points to the spring corresponding to the higher number. As the link is strictly straight, for a constant i every $\xi_{i,s}$ axes are parallel to each other. For the sake of simplicity we will denote them by ξ_i. In the stress-free state of the linkage the corresponding axes of every section point to the same direction. The bending moment, which creates the initial torus, is parallel with the axis ζ, so in the non-twisted torus the links are lying in the common $\xi\eta$ plane. The second level of reference systems is the only global $[xyz]$ system. We will show later the best way to choose it.

The homogenous cross-section of the linkage ensures that the linkage's shape does not change if we rotate every cross section by the same angle around the tangential of rod. The discretization has no effect on this property, i.e. we may rotate every cross-section (and its local reference system) around its ξ_i axis without any changes in the rod's spatial shape. So we get configurations after bending to a ring, where every $\xi\eta$ plane close the same angle with the links' plane, or after the twist of end-sections we can turn every cross-section until the η component of the moment vector in a specified one will be equal to zero.

Since there is no load acting on the rod, and we do not deal with contacts, therefore in an arbitrary part of rod the inner forces acting on both ends must be in equilibrium. That means that the resultant of stresses in any cross-section is the same, i.e. the stresses reduced to the origin of the global coordinate system give the same force $\mathbf{F}_0$ and moment $\mathbf{M}_0$ vectors in all sections. With other words, from a given pair of vectors $\mathbf{F}_0$ and $\mathbf{M}_0$ one can compute the inner forces in a cross-section by reducing the force and moment vector to that section. We do not need the force vector component of the reduced stresses, as the rod is treated inextensible and unshearable, so the strains will be computed only from the moment vector.

In the cross-sections of the links we need only the twist moment, since the link is infinitely stiff against bending. It is easy to show, that the twist moment is constant along one link.

Since the spring is infinitely stiff against twist, we need only the bending part of the moment vector to compute the deformation in the spring. The bending part of moment vector is orthogonal to the plane of two links connecting to the spring. The twisting part of moment vector (which is not the twist moment, and causes no twist deformation in the spring) is lying in this plane, and closes the same angle with the direction of link before and after the spring. So the twist moment (the projection of twisting moment to the link's direction) in the links before and after the spring will be the same.

(The last condition gives back the well-known result concerning the continuous model. According to that the twist moment in unloaded segments of rod is constant. This can be proven by a moment equation in the local reference system of rod: $M_\xi' + M_\eta M_\zeta (1/A - 1/B) = 0$, where A and B are the bending stiffness characteristics to the main inertial directions η and ζ. In case of a circular cross-section $A = B$, so the twist moment is constant.)

3. Computation of a model configuration

We want to determine the model shape for known:

- force and moment vectors $\mathbf{F}_0$ and $\mathbf{M}_0$, which are the inner forces reduced to the origin of $[xyz]$.
- vector $\mathbf{r}_0$ ($[xyz]$ position vector of the starting point of the first link).
- matrix $\mathbf{T}_{1,0}$, which transforms a vector given in the $[xyz]$ to the local reference system of the starting point of the first link.

Now we will show, how one can compute the state of $i+1$th link based on the state of the ith link, and of course, based on the vectors $\mathbf{F}_0$ and $\mathbf{M}_0$. (The following step corresponds to the ith step. We will use the numbering of elements as an index only where it is necessary.)

The $\mathbf{T}_{i,0}$ matrix consists of the unit vectors of the local co-ordinate axis of the starting point of the ith link:

$$\mathbf{T}_{i,0} = \begin{bmatrix} \xi_i^T \\ \eta_{i,0}^T \\ \zeta_{i,0}^T \end{bmatrix}.$$

The local co-ordinate system rotates around the ξ_i axis along the link by the angle $l\omega$. Here ω is the twist rate, computed from: $\omega = M_T/C$, where M_T is the twist moment:

$$M_T = \mathbf{M}^x \cdot \xi_i,$$

and $\mathbf{M}^x$ is the moment vector of inner forces in the global reference system at the end-point of the ith link. We already mentioned that the rotation around ξ_i has no effect on the ξ_i axis, so the co-ordinates of end-point can be computed from the starting point:

$$\mathbf{r}_i = \mathbf{r}_{i-1} + l\xi_i.$$

In the end point the local co-ordinate system can be computed by a rotation of $\mathbf{T}_{i,0}$ by $\mathbf{T}_1(l\omega)$. (A matrix $\mathbf{T}_j(\alpha)$ with only one lower index j means a rotation around the jth axis by the angle α.)

$$\mathbf{T}_{i,l} = \mathbf{T}_1(l\omega)\mathbf{T}_{i,0} = \begin{bmatrix} 1 & 0 & 0 \\ 0 & \cos(l\omega) & \sin(l\omega) \\ 0 & -\sin(l\omega) & \cos(l\omega) \end{bmatrix} \mathbf{T}_{i,0}.$$

We compute the moment vector of the end-section in the $[xyz]$ system:

$$\mathbf{M}^x = \mathbf{M}_0 + \mathbf{r}_i \times \mathbf{F}_0.$$

Subsequently we rotate $\mathbf{M}^x$ to the local system of the end-section:

$$\mathbf{M}^\xi = \mathbf{T}_{i,l}\mathbf{M}^x.$$

We would like to resolve this vector into a bending and a twisting moment, but the direction of the next rod is unknown, so the common plane of links is also unknown. The direction orthogonal

to this common plane is the direction of bending moment. The unit vector which points into this direction is denoted by $\mathbf{b}$. The system $[\xi_i, \eta_{i,l}, \zeta_{i,l}]$ has to be rotated around $\mathbf{b}$ to obtain the system $[\xi_{i+1}, \eta_{i+1,0}, \zeta_{i+1,0}]$. Since $\mathbf{b}$ is orthogonal to the ξ_i, it lies in the plane $\eta_{i,l}\zeta_{i,l}$. It can be computed, if we rotate the vector $\boldsymbol{\eta}_{i,l}$ around the axis ξ_i by the (unknown) angle φ (see Fig. 1). This transformation of the local co-ordinate system is denoted by the matrix $\mathbf{T}_1(-\varphi)$:

$$\mathbf{T}_1(-\varphi) = \begin{bmatrix} 1 & 0 & 0 \\ 0 & \cos(\varphi) & -\sin(\varphi) \\ 0 & \sin(\varphi) & \cos(\varphi) \end{bmatrix}.$$

In the third row of the matrix $\mathbf{T}_1(-\varphi)$ there are the local co-ordinates of the vector $\mathbf{b}$. In the second row there are the co-ordinates of the vector denoted by $\mathbf{w}$ in Fig. 1. The vector $\mathbf{w}$ is orthogonal to $\mathbf{b}$, so it lies in the plane of the ith and $(i+1)$th links.

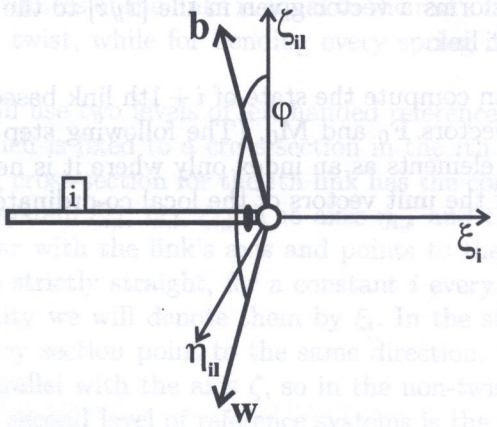

Fig. 1. Definition of angle φ

The projection of the moment vector to $\mathbf{b}$ is the bending moment M_B:

$$M_B = \mathbf{M}^{\xi} \cdot \mathbf{b},$$

which is proportional to the deformation of the spring:

$$\vartheta = \frac{M_B}{c}.$$

The co-ordinate system of the ith link has to be rotated by the angle ϑ around $\mathbf{b}$. This rotation will be performed in three steps. First we rotate around the tangential direction by the angle φ using the matrix $\mathbf{T}_1(-\varphi)$, then we rotate around the vector $\mathbf{b}$ by the angle ϑ using the matrix $\mathbf{T}_3(\vartheta)$, at last we turn back the system by φ. The matrix $\mathbf{T}_3(\vartheta)$ has the following form:

$$\mathbf{T}_3(\vartheta) = \begin{bmatrix} \cos(\vartheta) & \sin(\vartheta) & 0 \\ -\sin(\vartheta) & \cos(\vartheta) & 0 \\ 0 & 0 & 1 \end{bmatrix},$$

while the rotation backward by φ is performed via the matrix $\mathbf{T}_1(\varphi)$, which is the inverse of $\mathbf{T}_1(-\varphi)$. These steps are shown in Fig. 2, the axis of rotation is denoted by a double arrow, the axes after the turn are denoted by a thick line.

Now let us analyse the axes after the transformation $\mathbf{T}_1(-\varphi)$. Figure 3 shows the axes (b, w) after this rotation, and two other vectors: $\mathbf{t}$, and $\mathbf{n}$. Both of them are lying in the plane $[\xi_i, w]$. The direction of $\mathbf{t}$ is defined in such a way that it closes the same angle with the directions of both links.

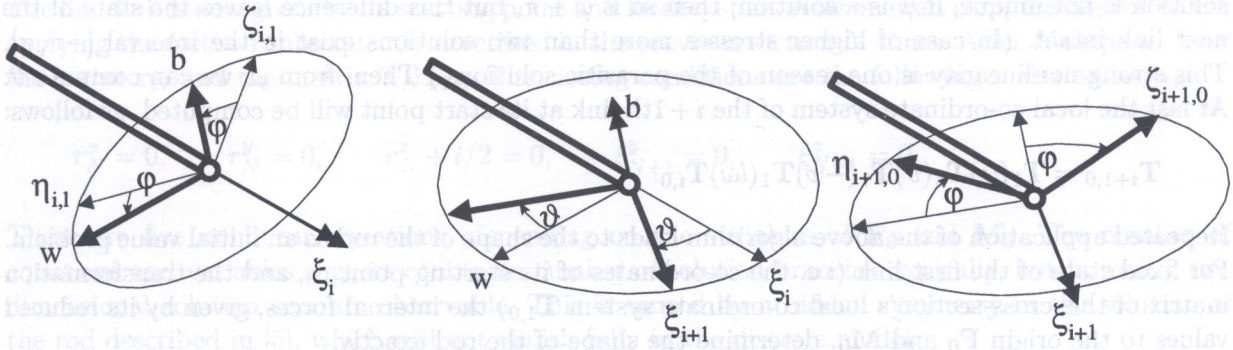

Fig. 2. Transformations of the local reference system

Observe that $\mathbf{n}$ is orthogonal to $\mathbf{t}$. Figure 3 shows that these direction can be computed from the vectors ξ_i and $\mathbf{w}$, if we rotate them around $\mathbf{b}$ by $\vartheta/2$. This transformation is denoted by $\mathbf{T}_3(\vartheta/2)$:

$$\mathbf{T}_3(\vartheta/2) = \begin{bmatrix} \cos(\vartheta/2) & \sin(\vartheta/2) & 0 \\ -\sin(\vartheta/2) & \cos(\vartheta/2) & 0 \\ 0 & 0 & 1 \end{bmatrix}.$$

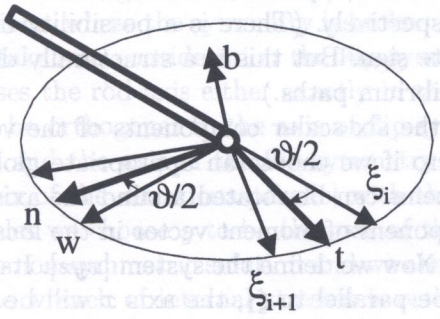

Fig. 3. Definition of the vectors $\mathbf{t}, \mathbf{n}$

This transformation makes possible to determine the value of φ. We resolve the moment vector into a bending and a twisting component. The first one is parallel to $\mathbf{b}$, the last one lies in the plane of the links. The twist moment is the same in both links, if the projections of the moment vector to ξ_i and ξ_{i+1} are equal to each other. Hence the bending moment is orthogonal to both links, the projections of the moment vector are the same as the projections of the twisting moment. These will be the same, if the twisting moment closes the same angle with ξ_i and ξ_{i+1}. This is only possible, if the twisting moment is parallel with $\mathbf{t}$. Hence both components of the moment vector are orthogonal to $\mathbf{n}$, the vector $\mathbf{M}$ is also orthogonal to $\mathbf{n}$, i.e., the second component of $\mathbf{M}$ in the co-ordinate system $[tnb]$ is zero:

$$\mathbf{e}_2^{\mathrm{T}} \cdot \mathbf{T}_3(\vartheta/2)\mathbf{T}_1(-\varphi)\mathbf{M}^{\xi} = 0,$$

where $\mathbf{e}_2^{\mathrm{T}}$ is the transpose of the second unit vector. Since the matrix $\mathbf{T}_3(\vartheta/2)$ depends on ϑ which in turn, is a function of φ, we can construct a function of φ, which must be zero:

$$f(\varphi) = -M_\xi \sin\frac{\vartheta(\varphi)}{2} + (M_\eta \cos\varphi - M_\zeta \sin\varphi)\cos\frac{\vartheta(\varphi)}{2} = 0.$$

We have to solve this nonlinear equation for φ. The first derivative of function f can be derived analytically as a function of φ, so the solution can be found by a simple Newton-iteration. The

solution is not unique, if φ is a solution, then so is $\varphi + \pi$, but this difference leaves the state of the next link intact. (In case of higher stresses more than two solutions exist in the interval $[-\pi, \pi]$. This strong nonlinearity is one reason of the parasitic solutions.) Then, from φ, we can compute ϑ. At last the local co-ordinate system of the $i+1$th link at its start point will be computed, as follows:

$$\mathbf{T}_{i+1,0} = \mathbf{T}_1(\varphi)\mathbf{T}_3(\vartheta)\mathbf{T}_1(-\varphi)\mathbf{T}_1(l\omega)\mathbf{T}_{i,0}.$$

Repeated application of the above algorithm leads to the shape of the rod as an initial value problem. For fixed state of the first link (i.e. the co-ordinates of its starting point $\mathbf{r}_0$, and the transformation matrix of this cross-section's local co-ordinate system $\mathbf{T}_{1,0}$) the internal forces, given by its reduced values to the origin $\mathbf{F}_0$ and $\mathbf{M}_0$, determine the shape of the rod exactly.

4. Closing conditions

A rod shape is acceptable as a solution of the boundary value problem if and only if the axes of the 1st and $(N+1)$st links coincide (the axes η and ζ can be different), i. e.

- their starting points have the same co-ordinates,
- their axes ξ have the same direction.

The axis ξ of a link is given by the first row of the transformation matrix of the local reference system. The $\boldsymbol{\xi}$ vectors are unit vectors, so the $\boldsymbol{\xi}$ vectors of two links are parallel if the first and second coordinates are equal, respectively. (There is a possibility of parasitic solutions, when the third co-ordinate has the opposite sign. But this is a structurally different solution, which will be filtered out from the global equilibrium paths.)

The rod shape is defined by the six scalar components of the vectors $\mathbf{F}_0$ and $\mathbf{M}_0$, but one of these variables can always be zero if we choose an appropriate global reference system. We have seen that the local reference systems can be rotated around the axis ξ. We choose this rotation in such a way, that the second component of moment vector in the local system (i.e. M_η) will be zero in the mid-point of the first link. Now we define the system $[xyz]$. Its origin will be in the mid-point of the first link, the axis z will be parallel to ξ_1, the axis x will be parallel to $\eta_{1,l/2}$, and the axis y will be parallel to $\zeta_{1,l/2}$. Thus the second co-ordinate of $\mathbf{M}_0$ will be always zero. The connection between the global and local systems is described by a matrix $\mathbf{T}$, which has the following form in the mid-point of the first link:

$$\mathbf{T}_{1,l/2} = \begin{bmatrix} 0 & 0 & 1 \\ 1 & 0 & 0 \\ 0 & 1 & 0 \end{bmatrix},$$

while the co-ordinates of the start-point of first link are:

$$\mathbf{r}_0 = \begin{bmatrix} 0 & 0 & -l/2 \end{bmatrix}^T.$$

Hence z is parallel to ξ_1, the third co-ordinate of $\mathbf{M}_0$ is the twist moment (M_T). Now the twist rate can be computed, which is constant along the whole rod, since the twist moment is also constant. Then the transformation matrix of the starting point is computed via a rotation around the first axis by $l\omega/2$:

$$\mathbf{T}_{1,0} = \begin{bmatrix} 1 & 0 & 0 \\ 0 & \cos\dfrac{l\omega}{2} & -\sin\dfrac{l\omega}{2} \\ 0 & \sin\dfrac{l\omega}{2} & \cos\dfrac{l\omega}{2} \end{bmatrix} \mathbf{T}_{1,l/2}.$$

The first link is now given by its starting point and local system. Now one can compute the rod shape applying the method subsequently described in the previous section N times. After N steps we have the vector $\mathbf{r}_N$ and the matrix $\mathbf{T}_{N+1,0}$. The closing conditions are the following scalar equations:

$$r_N^x = 0, \qquad r_N^y = 0, \qquad r_N^z + l/2 = 0, \qquad \xi_{N+1}^y = 0, \qquad \xi_{N+1}^z = 0.$$

These are five nonlinear equations, depending on the variables of $\mathbf{F}_0$ and $\mathbf{M}_0$. The number of equations and variables suggest countable number of solution branches typically, but in reality two dimensional solution sets are observable. This is caused by a hidden symmetry in the solution of the rod described in [5], which will not vanish fully in the discrete model.

One possibility to find equilibrium paths is skipping one condition, finding equilibrium paths and then filtering out the spurious solutions, where the skipped condition is not fulfilled. In the discrete model we recommend skipping the third condition, so the ratio of error to the length of a link can be seen in the rod shape in any projection. (If we skipped one of the first two conditions, the error ratio would depend on the direction of the projection, while skipping one of the last two conditions would lead to a discontinuity in the spring, which is added to the discontinuity from the moment.)

Another possibility is the application of the flip-symmetry of the continuous model. Domokos and Healey [5] showed that there is always an axis of C_2 symmetry of the rod axis. The continuous rod axis intersects orthogonally this axis in two points, the difference in the arc-length parameter of these points is $L/2$. The wrench, computed from the $\mathbf{F}_0$ and $\mathbf{M}_0$ intersects orthogonally the axis of this flip-symmetry. The discrete model gives a better approximation if this C_2 symmetry remains. (However non-symmetric solutions, where the symmetry is broken by the discretization will be lost). There are two possibilities to take into consideration the flip-symmetry in the discrete model. The axis of the flip-symmetry crosses the rod axis either exactly in the middle of a link or at a spring. In the first case the link must be orthogonal to the axis of flip-symmetry, in the second case both links connecting to the spring and the axis of the flip-symmetry lying in one plane, and the axis of the symmetry is the bisectrix of the directions parallel with the connecting links pointing away from the spring. In our examples we choose y to be the axis of the flip-symmetry, so the first link fulfills the flip-symmetry in the non-symmetric solution and we can use the same starting conditions in the symmetric solution. The wrench of internal stresses is orthogonal to y, if and only if the y co-ordinates of $\mathbf{F}_0$ and $\mathbf{M}_0$ are zeroes (M_{0y} was in the non-symmetric solution also 0). So the rod shape is defined by four variables: F_{0x}, F_{0z}, M_{0x}, M_{0z}. The closing conditions depend on the parity of the number of links.

In case of even number of links ($N = 2k$) we compute $\mathbf{r}_k$ and $\mathbf{T}_{k+1,0}$ by repeating the method of previous section k times. The middle of the kth link must lie on the axis y, and ξ_{k+1} must be orthogonal to the axis y. So we can form the following three conditions:

$$\begin{aligned} r_k^x + \tfrac{l}{2}\xi_{k+1}^x &= 0, \\ r_k^z + \tfrac{l}{2}\xi_{k+1}^z &= 0, \\ \xi_{k+1}^y &= 0. \end{aligned}$$

In case of odd number of links ($N = 2k - 1$) we compute $\mathbf{r}_k$, $\mathbf{T}_{k,0}$ and $\mathbf{T}_{k+1,0}$ by repeating the method of previous section k times. The kth spring must lie on the axis y, and the sum of unit vectors parallel with links before and after this point must orthogonal to the axis y. This leads to the following three conditions:

$$\begin{aligned} r_k^x &= 0, \\ r_k^z &= 0, \\ \xi_k^y + \xi_{k+1}^y &= 0. \end{aligned}$$

5. Computation of equilibrium paths

We want to find all equilibrium paths (all equilibrium states, where the shape has C_2 symmetry) of the ring in a given domain of parameters. The difference between the number of the parameters and the number of equations suggests the application of the simplex algorithm [7]. The main idea of this method is that we divide the parameter space to simplices, which fill out the given domain. We check every simplex, whether the equilibrium path has a section inside this simplex or not. In order to do this we compute the error of closing conditions in the vertices of simplex. Then we linearize the functions with the values in the vertices, which leads to a line as a solution. If there is a section of this line inside the simplex, it crosses two sides of simplex. The section between these points is considered as a linearized equilibrium path of the ring. This computation on all simplices of the parameter space leads to all parts of equilibrium path. For large space and small simplices (which is necessary to a good approximation) the computation effort is very large. The possibilities to speed-up computing are the parallelisation and the organization the order of computed simplices. More information about these methods is presented in [7] and [6].

We used the serial version of the simplex algorithm (i.e. only one computer with one processor was used) with the parameters and functions presented in the previous section. Here we show some results.

The dimension of lengths was chosen to have a rod with unit length ($L = 1$), and the dimension of forces was chosen in order to have $A = 1$. The twist stiffness has no effect on the equilibrium paths, only on the twist rate and the stability of the solution. At this point of the research we are not interested in the stability of solutions. The twist rate is computed from the twist moment via $\omega = M_T/C$.

The scanned interval of variables were: $F_x = -250..251$; $F_z = -190..124$; $M_x = -25, 5..26, 5$; $M_z = -0, 3..40, 5$. The parameter space was divided into $200 \times 100 \times 100 \times 102$ cubes, and each cube to $4! = 24$ simplices.

In this paper we present only symmetric solutions. Figure 4 shows equilibrium paths of a rod with 8 links. Hence the solution uses the flip-symmetry, the rod shape is defined by 4 parameters, therefore the equilibrium paths are in a 4 dimensional space. The diagrams are 2 dimensional projections of this space. Figures 4a-d are projections parallel with the plane of 2-2 co-ordinate axes.

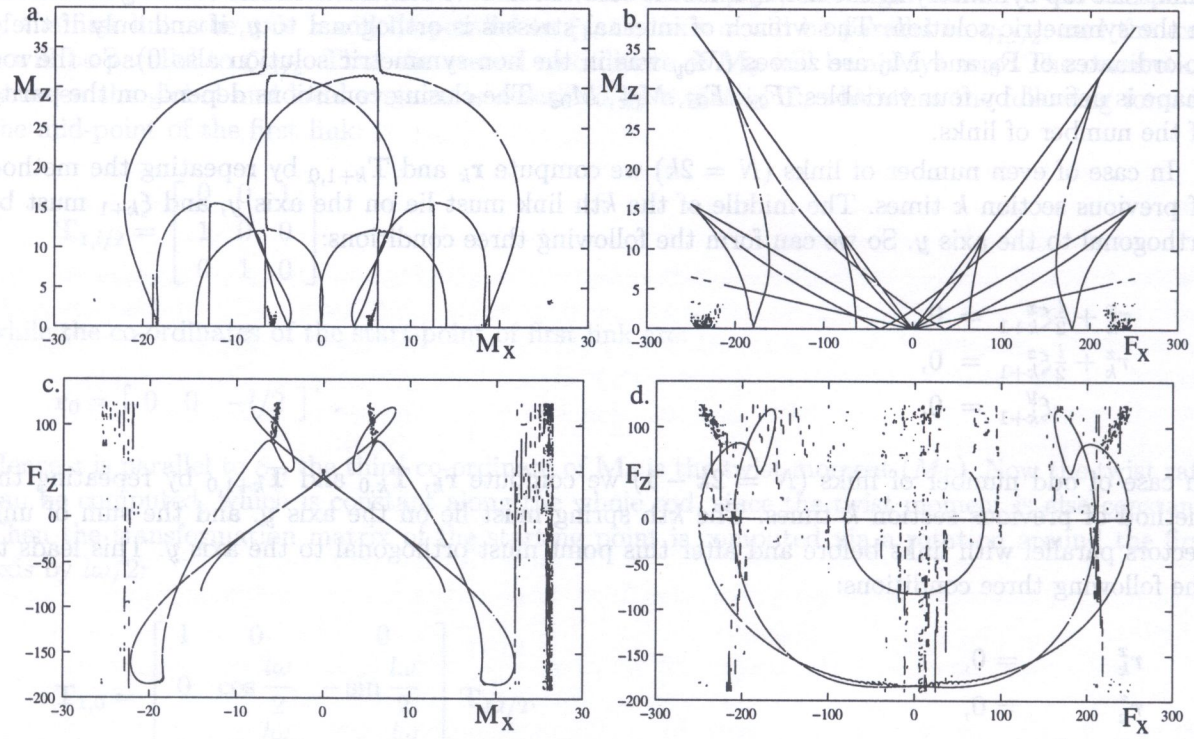

Fig. 4. Equilibrium paths for $N = 8$

The vertical axis in the upper diagrams (a, b) is M_z (i.e. the twist moment), in the lower diagrams (c, d) F_z (i.e. the normal force in the first link). The horizontal axis in the left diagrams (a, c) is the M_x moment, in the right diagrams (b, d) the F_x force. The computation was performed only for positive twist moments. For negative values we should mirror the upper diagrams to the horizontal axis. In the lower diagrams we would have the same lines behind or before the existing lines.

First we will analyze the equilibrium paths corresponding to the trivial shapes. In continuous model these are planar rings, with or without overlapping. On diagram (a) these paths are vertical lines at $M_x = 2k\pi$, where k is non-zero integer. On diagram (b) the trivial paths are straight lines through the origin of co-ordinate system. The highest slope corresponds to the simplest shape (without overlapping), the smaller slopes are the paths of "overlapping" shapes, even if the overlapping does not occur in all cases by the discrete model. Since there is no normal force in the ring, the trivial paths are points on the diagram (c). The non-trivial paths bifurcate from these points, that is why we do not see only points. On diagram (d) the trivial paths are overlapping lines on the horizontal co-ordinate axis.

The next objects of our analysis are the bifurcations. Since the simplex method gives maximum 2 solutions on the faces of a simplex, the bifurcation fall apart, and we cannot see any bifurcation point. This effect can be decreased by using smaller simplices (and larger computation time, of course). Below we will speak about the bifurcations as we had compute thus region with zero mesh-size (which join the aparted paths as a limit).

Figure 5 shows a part of Fig. 4a. There are six points selected at the same twist rate ($M_T = 10.5$). The corresponding shapes of the ring is presented in Fig. 6. Shapes a and b are trivial (planar), shapes c and d are lying on the first bifurcation branch. They can be transformed into each other via rigid body motions, because the shape has a second axis of flip-symmetry. The shapes e and f are lying on the secondary non-trivial branches.

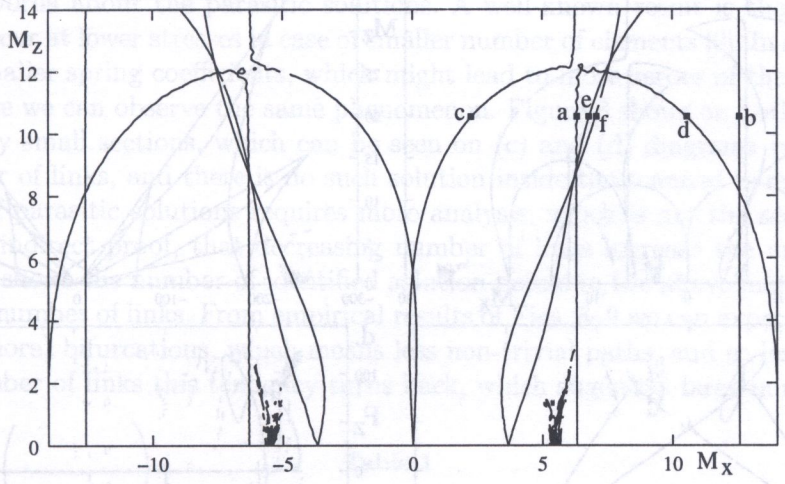

Fig. 5. Part of Fig. 4a

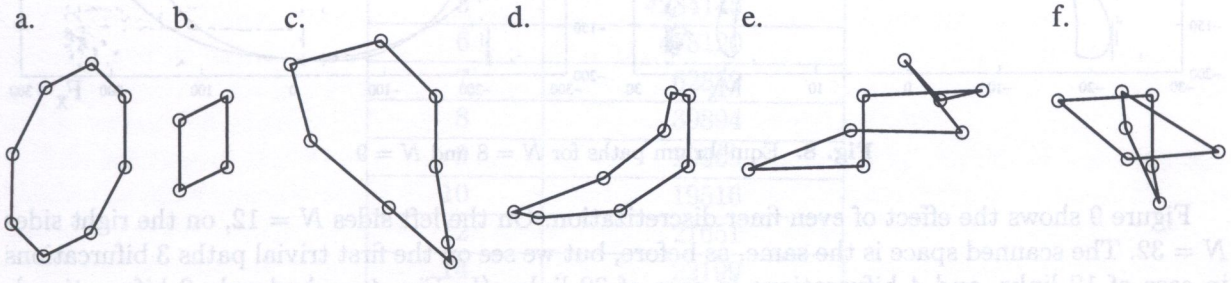

Fig. 6. Shapes at $M_T = 10.5$ on Fig. 5

Figure 7 shows a sequence of shapes, lying on the first non-trivial branch. The first one is the trivial shape at the critical twist moment. In the next shapes the twist moment is decreasing until the last one, where the twist moment is equal to zero; this is an 8-shape figure on the right side of the sequence.

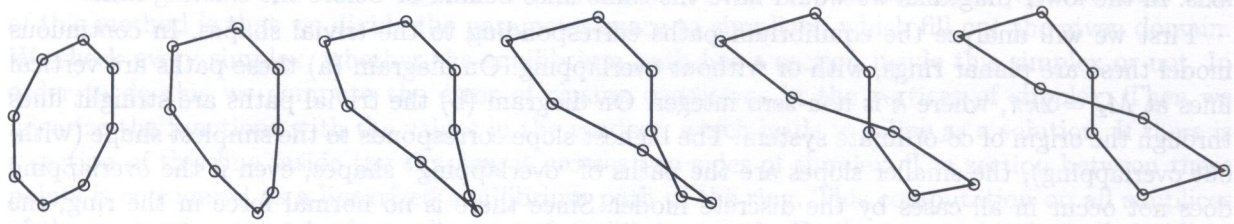

Fig. 7. Shapes on the first nontrivial branch

Since the discrete model is an approximate solution of the continuous model, we analyze the effect of the number of links. Figure 8 shows the equilibrium paths of a rod with 8 and 9 links. Since the diagrams are symmetric to the vertical axis, we present only half of them, on the left sides the results for $N = 8$, on the right sides the results for $N = 9$. We can observe that in case of higher number of links the bifurcations occur at lower values of twist. In the links of rod with $N = 8$ the difference between the continuous rod and the approximate solution is higher, and the geometrical constraint that makes the links straight makes the rod stiffer. Other result of the finer discretization, that the fourth trivial path is also present. In case of $N = 8$ this would lead to eight overlapping links, where twist moment could occur only at infinity force F_x.

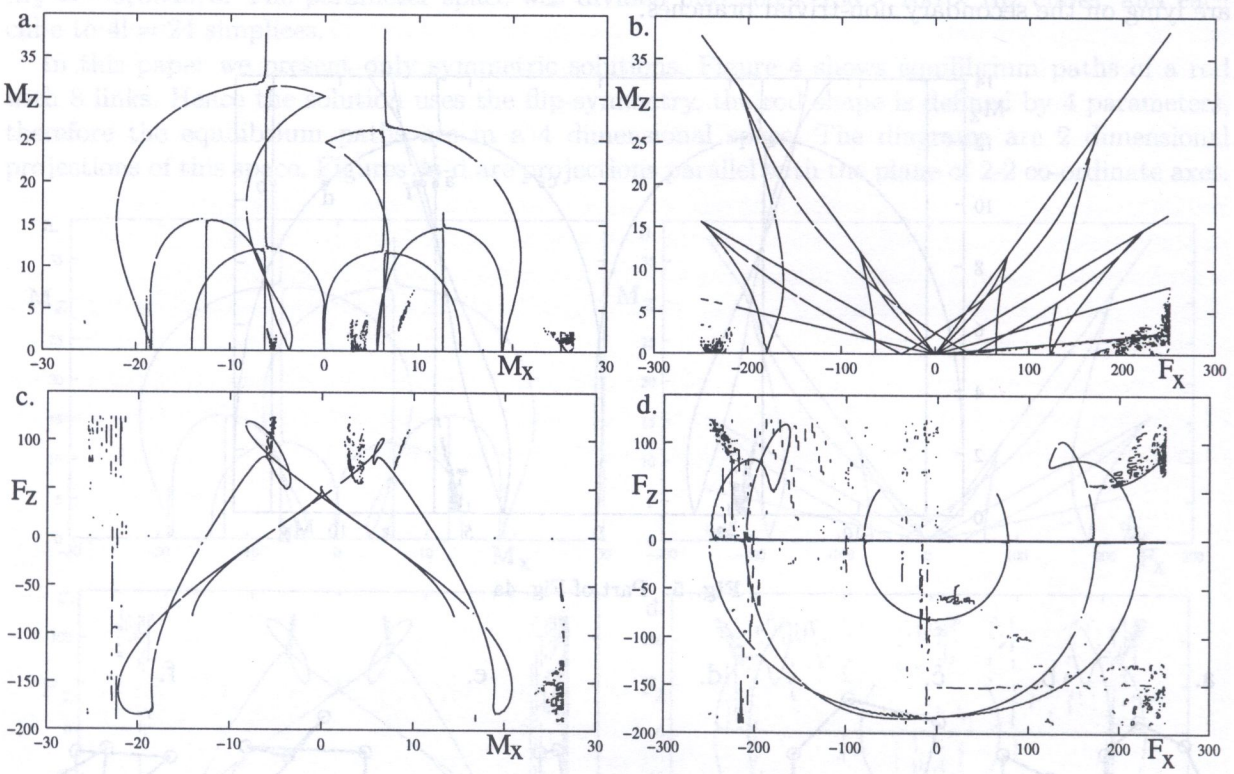

Fig. 8. Equilibrium paths for $N = 8$ and $N = 9$

Figure 9 shows the effect of even finer discretization. On the left sides $N = 12$, on the right sides $N = 32$. The scanned space is the same, as before, but we see on the first trivial paths 3 bifurcations in case of 12 links, and 4 bifurcations in case of 32 links. (In Fig. 4 we had only 2 bifurcations). Further increasing number of links converges to the continuous solution.

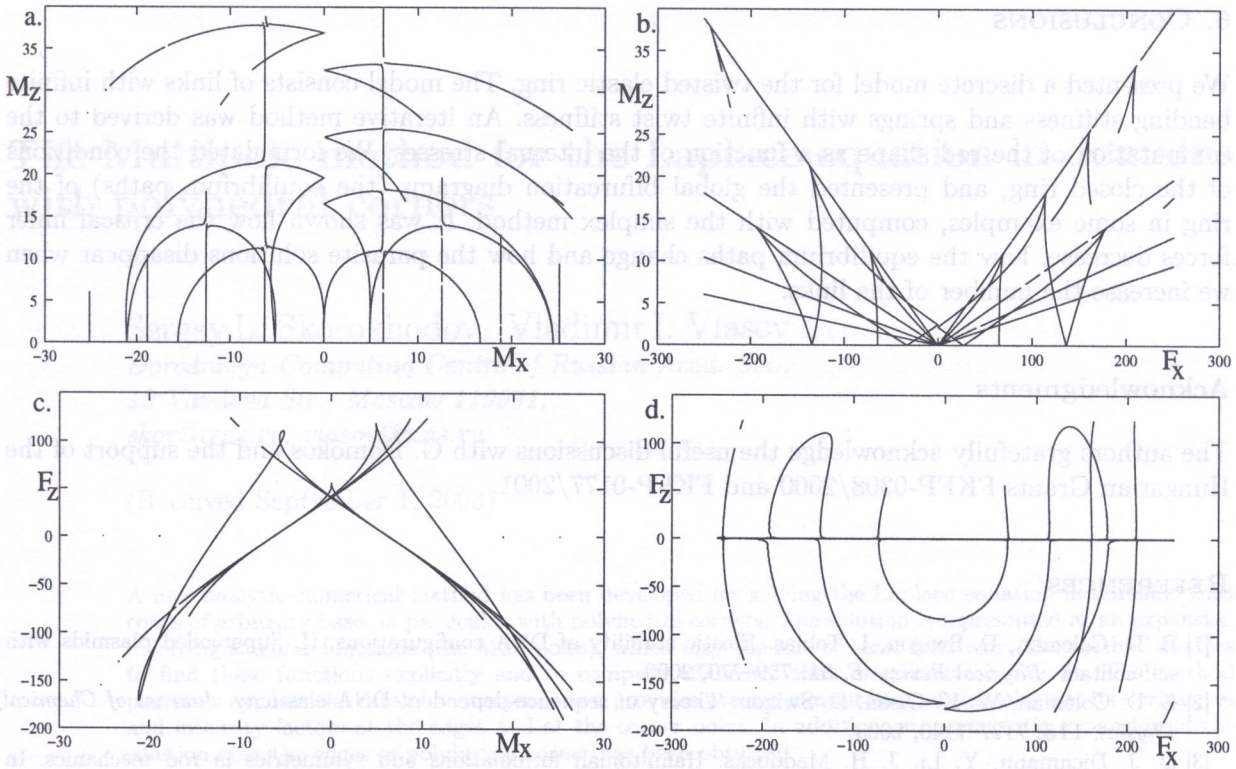

Fig. 9. Equilibrium paths for $N = 12$ and $N = 32$

At last some words about the parasitic solutions. A well-known result is that the parasites in discrete models occur at lower stresses in case of smaller number of elements [9]. In our case the larger elements mean smaller spring coefficients, which might lead to more zeroes of the function f in the interval $[0, \pi]$. Here we can observe the same phenomenon. Figure 8 shows on both sides (for $N = 8$ and $N = 9$) messy small sections, which can be seen on (c) and (d) diagrams very well. Figure 9 has higher number of links, and there is no such solution inside the scanned parameter space. The systematization of parasitic solutions requires more analysis, which is not the scope of this paper. We just show an indirect proof, that decreasing number of links increase the number of parasite solutions. Table 1 shows the number of identified solution points in the above mentioned parameter space for variable number of links. From empirical results of Figs. 8–9 we can expect for less links less (or, anyway not more) bifurcations, which means less non-trivial paths, and so less solution points. But for small number of links this tendency turns back, which suggest a large number of parasites.

Table 1

No. of links	No. of solution points
4	5216532
5	4284145
6	478120
7	62889
8	39894
9	29969
10	19516
12	21651
14	22199
16	22148

6. Conclusions

We presented a discrete model for the twisted elastic ring. The model consists of links with infinite bending stiffness and springs with infinite twist stiffness. An iterative method was derived to the computation of the rod shape as a function of the internal stresses. We formulated the conditions of the closed ring, and presented the global bifurcation diagrams (the equilibrium paths) of the ring in some examples, computed with the simplex method. It was shown how the critical inner forces decrease, how the equilibrium paths change and how the parasite solutions disappear when we increase the number of the links.

Acknowledgments

The authors gratefully acknowledge the useful discussions with G. Domokos and the support of the Hungarian Grants FKFP-0308/2000 and FKFP-0177/2001.

References

[1] B. D. Coleman, D. Swigon, I. Tobias. Elastic stability of DNA configurations. II. Supercoiled plasmids with self-contact. *Physical Review E*, **61**: 759–770, 2000.

[2] B. D. Coleman, W. K. Olson, D. Swigon. Theory of sequence-dependent DNA elasticity. *Journal of Chemical Physics*, **118**: 7127–7140, 2003.

[3] D. J. Dichmann, Y. Li, J. H. Maddocks. Hamiltonian formulations and symmetries in rod mechanics. In J. P. Mesirov, K. Schulten, D. W. Sumners, eds., *Mathematical Approaches to Biomolecular Structure and Dynamics*, 71–113, Springer, New York, 1996.

[4] G. Domokos. A group theoretic approach to the geometry of elastic rings. *J. Nonlinear Science*, **5**: 453–478, 1995.

[5] G. Domokos, T. Healey. Hidden symmetry of global solutions in twisted elastic rings. *J. Nonlinear Science*, **11**: 47–67, 2001.

[6] G. Domokos, I. Szeberényi. A parallel hybrid approach to nonlinear boundary value problems. *Computer Assisted Mechanics and Engineering Sciences*, **11**: 15–34, 2004.

[7] Zs. Gáspár, G. Domokos, I. Szeberényi. Parallel algorithm for the global computation of elastic bar structures. *Computer Assisted Mechanics and Engineering Sciences*, **4**: 55–68, 1997.

[8] Zs. Gáspár, R. Németh. A special shape of a twisted ring. *Proc. of 2nd European Conference on Computational Mechanics*, CD p. 11, 2001.

[9] G. Károlyi, G. Domokos. Symbolic Dynamics of infinite depth: finding global invariants for BVPs. *Physica D*, **134**: 316–336, 1999.

[10] D. Swigon, B. D. Coleman, I. Tobias. The elastic rod model for DNA and its application to the tertiary structure of DNA minicircles and mononucleosonmes. *Biophysical Journal*, **74**: 2515–2530, 1998.

[11] J. M. T. Thompson, G. H. M. van der Heijden, S. Neukirch. Super-Coiling of DNA-Plasmids: the Generalised Ply. *Proc. R. Soc. Lond., Series A*, **458**: 959–985, 2001.